Dalton Transactions

ROYAL SOCIETY OF CHEMISTRY

COMMUNICATION

View Article Online
View Journal | View Issue

Cite this: *Dalton Trans.*, 2025, **54**, 10868

Received 30th May 2025,
Accepted 25th June 2025

DOI: 10.1039/d5dt01271f

rsc.li/dalton

Mechanism of catalyst activation in iron(porphyrin)-catalysed aerobic oxidative cleavage of 2,3-dimethylindole†

Anna C. Brezny, *[a] James H. Lyke,[a] Sigrid E. Olsen,[a] Emma R. Straton[b] and Olha Zubarieva[a]

Ferric porphyrins catalyse the aerobic oxidative cleavage of 2,3-dimethylindole, mimicking dioxygenase enzymes. The data herein suggest that the indole reduces the Fe^{III}(porphyrin) to Fe^{II}(porphyrin) *via* a proton-coupled electron transfer mechanism. Subsequently, Fe^{II}(porphyrin) binds O_2 and generates the critical superoxo intermediate, which oxidatively cleaves a second equivalent of substrate.

Tryptophan 2,3-dioxygenase (TDO) and indolamine 2,3-dioxygenase (IDO), the two dioxygenase enzymes in humans, catalyse the first steps in the kynurenine pathway. This pathway is responsible for L-tryptophan metabolism to nicotinamide adenine dinucleotide (NAD^+), and its dysregulation is involved in major health issues including cancer, inflammatory disorders, neurodegenerative diseases, and psychiatric disorders.[1–3] As part of this pathway, both TDO and IDO catalyse the oxidative cleavage of L-tryptophan to *N*-formylkynurenine (Scheme 1).[4]

Common biomimics of heme-containing enzymes use iron porphyrin complexes such as Fe(TPP) (TPP = *meso*-tetraphenylporphyrin).[4] Synthetic metalloporphyrins are known to activate O_2, and are often used in the context of the oxygen reduction reaction.[5–9] Stahl recently reported the use of O_2-derived metal–oxos to achieve dioxygenase reactivity.[10]

Fe(TPP) has been used with indole substrates in order to mimic TDO and IDO. Both dioxygenase enzymes are thought to oxidize the substrate *via* an iron superoxo intermediate ($Fe^{III}(O_2^{\bullet-})$).[11–14] In order to provide more evidence that the active oxidant is $Fe^{III}(O_2^{\bullet-})$, recent work from the Goldberg and Wijeratne labs demonstrated that synthetic iron porphyrin superoxo complexes can oxidatively cleave indoles in a stoichiometric fashion.[15,16] These elegant studies showed that at low temperatures the $Fe^{III}(O_2^{\bullet-})$(TPP) complexes react with 2,3-dimethyl-1*H*-indole (2,3-DMI, **1**) (Scheme 2). More specifically, the superoxo complex oxidatively cleaves the C=C and generates *N*-(2-acetyl-phenyl)-acetamide (**2**) in moderate (49%[15] and 31%[16]) yields. Wijeratne showed that the cleavage reactions occur faster with electron-poor iron porphyrins such as Fe(PFPP)(L) (PFPP = *meso*-pentafluorophenylporphyrin).

Work from Dey and coworkers explored a catalytic oxidative cleavage of 2,3-dimethylindole by an iron picket fence porphyrin attached to a self-assembled monolayer-modified gold electrode.[17,18] Using *in situ* resonance Raman spectroscopy, they demonstrated that under these electrochemical conditions, the $Fe^{III}(O_2^{\bullet-})$(porphyrin) is the active oxidant as well. In all of these aforementioned biomimetic systems, 2,3-dimethylindole serves as a model substrate due to its rapid reaction with the iron superoxo species.

We were interested in further exploring the reactivity of FePFPP with indole substrates. Surprisingly, upon combining Fe^{III}(PFPP)Cl with 2,3-dimethylindole in air, we observed formation of the cleavage product **2** in 35% yield assuming 1 : 1 stoichiometry (Scheme 3). This reactivity was unexpected because the iron porphyrin was added to the reaction in the +3 oxidation state, but superoxo complexes are generated from reaction of O_2 with an iron site in the +2 oxidation state. Intrigued by this result, we sought to understand how this unexpected reactivity could occur.

One key observation was that during the reaction, the solution visually changed from a green-brown color to a bright red, suggesting a change in metal oxidation state. In order to inves-

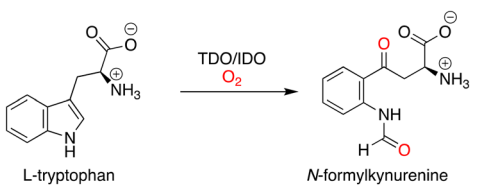

Scheme 1 Enzyme-catalysed oxidative cleavage of L-tryptophan to yield *N*-formylkynurenine.

[a]*Department of Chemistry, St. Olaf College, Northfield, MN 55057, USA. E-mail: brezny1@stolaf.edu*
[b]*Department of Chemistry, Skidmore College, Saratoga Springs, NY 12866, USA*
† Electronic supplementary information (ESI) available. See DOI: https://doi.org/10.1039/d5dt01271f

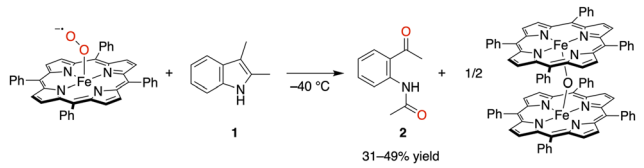

Scheme 2 Goldberg and Wijeratne demonstrated the stoichiometric oxidation of indoles with $Fe^{III}(O_2^{\bullet-})$(TPP) complexes.

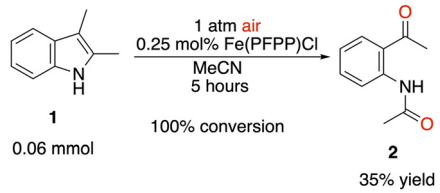

Scheme 3 The aerobic oxidation of **1** catalysed by Fe^{III}(PFPP)Cl leads to the formation of **2**.

tigate this observation quantitatively, *in situ* UV-Vis spectra were used to interrogate the catalyst resting state. We compared the catalytic reaction spectra to those of independently prepared Fe^{III}(PFPP)Cl and $Fe^{III}(O_2^{\bullet-})$(PFPP)(L) complexes, where L is presumably acetonitrile solvent. The *in situ* spectra revealed that the majority of iron during catalysis is in the form of the superoxo complex (Fig. 1). The presence of the $Fe^{III}(O_2^{\bullet-})$(PFPP)L complex is consistent with the observed red color. This is a surprising result because only iron(III) was used and no reductant was added to the reaction mixture, yet only iron(II) binds dioxygen.

In order to understand how the superoxo species was being generated during catalysis, we considered several possible mechanisms. The first was a photocatalytic reaction for dioxygen activation and substrate oxidation. Several studies with metalloporphyrins have proposed the formation of a superoxo where the M^{III}(P) undergoes photoexcitation, followed by intersystem crossing to form a relatively long-lived excited state. This complex then binds O_2 to generate a M^{IV}-superoxo complex, which is proposed to oxidize substrates.[19–24] We compared the yields when the reaction vessel was exposed to ambient light, blue LEDs, white LEDs, and kept dark. The reactions all gave full conversion and 35% yield of the oxidative cleavage product in 5 hours.

After ruling out a photocatalytic mechanism, we next considered a mechanism in which 2,3-DMI was serving as the reductant. In order to test this hypothesis, we reacted the Fe^{III}(PFPP)Cl with excess 2,3-DMI in the absence of O_2. The resulting UV-Vis spectrum gave a spectroscopic signature in the Q-band region that matched independently prepared ferrous porphyrin (Fig. 2). Essentially, the reaction of Fe^{III}(PFPP)Cl and 2,3-DMI leads to the formation of Fe^{II}(PFPP)(L) and an indole-derived byproduct. This result demonstrates that the first equivalent of 2,3-DMI sacrificially reduces the ferric porphyrin. Then under catalytic conditions, the resulting ferrous porphyrin can bind O_2 to generate the superoxo complex resting state. This in turn oxidizes the *second* equivalent of 2,3-DMI.

However, simple outer-sphere reduction of the metal by the indole is thermodynamically unfavourable based on the reduction potential of the oxidized indole (1.1 V *vs.* SCE)[25] compared to the iron porphyrin (−0.37 V *vs.* $Fc^{+/0}$ or 0.01 V *vs.* SCE). Moreover, we observed the same catalytic activity when using iron tetraphenylporphyrin chloride (Fe(TPP)Cl) which is even harder to reduce.[26] In either case, the minimum barrier (25 kcal mol^{-1}) is inconsistent with the observed reaction rate (full conversion in 5 hours).

Although outer-sphere electron transfer is infeasible, it is possible that the reduction instead occurs through a proton-

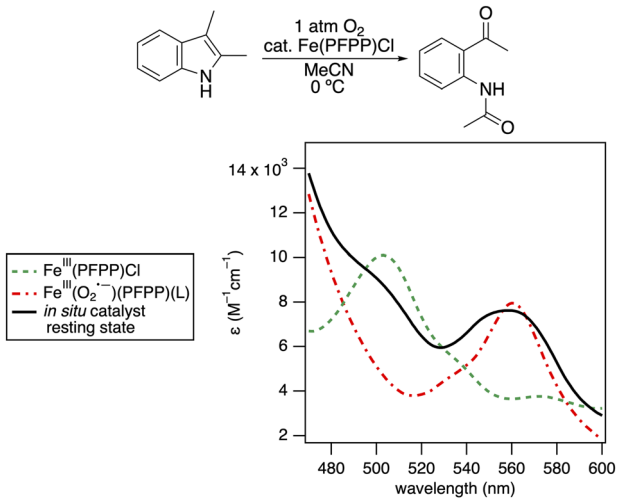

Fig. 1 UV-Vis spectrum of Q-bands of catalyst during the oxidative cleavage of 2,3-dimethyl indole (black) compared to genuine Fe(PFPP)Cl (green) and $Fe(O_2^{\bullet-})$(PFPP) (red).

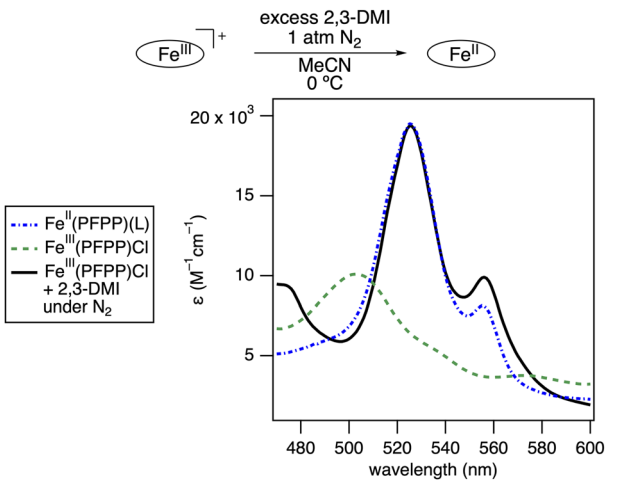

Fig. 2 UV-Vis spectrum of Q-bands of Fe^{III}(PFPP)Cl reacted with excess 2,3-DMI in the absence of O_2 (black) compared to genuine Fe^{III}(PFPP)Cl (green) and Fe^{II}(PFPP)(L) (blue).

coupled electron transfer (PCET) mechanism, generating a neutral indole radical (**3**) (Scheme 4). Consistent with this hypothesis, we isolated the major byproduct **4** from a large-scale reaction. This compound is a known dimerization product from neutral indole radicals reacting in the presence of dioxygen.[27–30] The formation of **3** is tentatively proposed based on the isolation of **4** from the reaction mixture.

In order to provide evidence for the proposed PCET mechanism, we synthesized 1-methyl-2,3-dimethyl-1*H*-indole (*N*-methyl-DMI), a substrate in which the N–H has been replaced with an N–Me. Consistent with our hypothesis, mixing *N*-methyl-DMI with Fe^{III}(PFPP)Cl in an N_2 atmosphere showed no reaction by UV-Vis (Fig. 3). In contrast to the reaction with **1**, we did not observe the formation of the ferrous Fe^{II}(PFPP)(L). Additionally, under catalytic conditions in the presence of O_2, no reaction of the *N*-methyl-DMI was observed—only starting material was recovered (100% NMR yield).

Cyclic voltammetry studies were used to estimate the oxidation potential of 2,3-DMI and *N*-methyl-DMI. Although the voltammograms are chemically irreversible, the onset potential for the methylated indole is similar to that of 2,3-DMI (Fig. 4). If a simple outer-sphere electron transfer were operative, *N*-methyl-DMI would be able reduce Fe^{III}(PFPP)Cl. Instead, the fact that the methylated indole cannot reduce the ferric porphyrin provides evidence that the N–H proton is critical, consistent with a PCET mechanism.

A deuterated substrate provided further evidence supporting the N–H being critical in the reduction of the ferric porphyrin. The deuterated analogue of the substrate, 2,3-dimethyl-1*H*-indole-1-*d* (**1-D**), was synthesized and subjected to the catalytic reaction conditions. The deuterium was observed

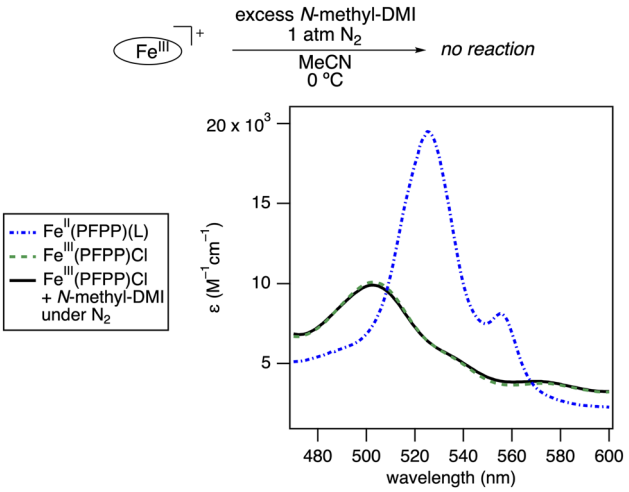

Fig. 3 UV-Vis spectrum of Q-bands of Fe^{III}(PFPP)Cl reacted with excess *N*-methyl-DMI in the absence of O_2 (black) compared to genuine Fe^{III}(PFPP)Cl (green) and Fe^{II}(PFPP)(L) (blue).

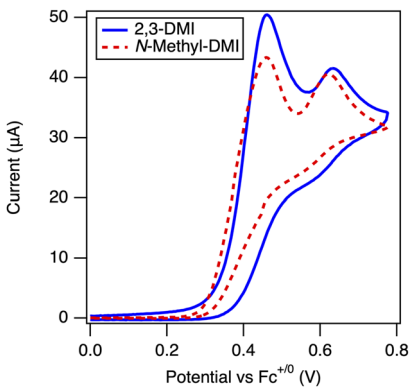

Fig. 4 Cyclic voltammograms of 2,3-DMI (blue) and *N*-methyl-DMI (red) in 0.1 M $[NBu_4][PF_6]$ in acetonitrile with 100 mV s^{-1} scan rate.

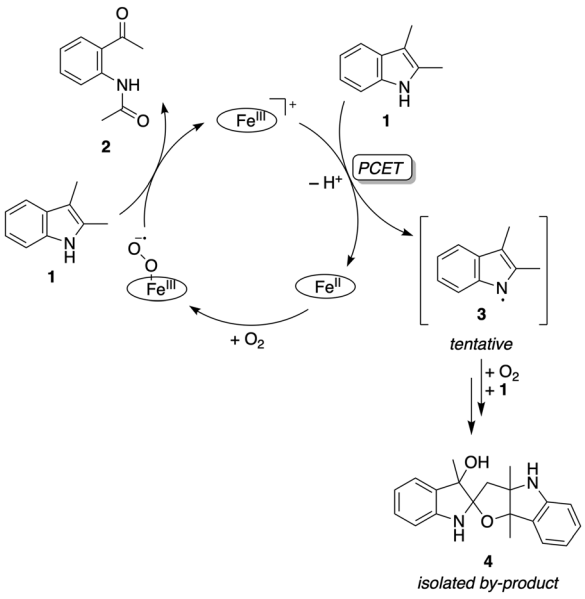

Scheme 4 Proposed PCET mechanism for the generation of Fe^{II}(PFPP)L in the absence of reductant. The tentatively proposed neutral indole radical (**3**) is known to react with O_2 to generate the isolated side product, dimer **4**.

to scramble into the methylene and methyl group of the dimer product (**4-D**) (Scheme 5). This observation could not be explained by simple acid/base exchange with solvent. Instead, it is more consistent with a PCET mechanism in which the H/D-atom from the nitrogen is lost as part of the reduction of the metal (Scheme 6).

The combination of these results helps to explain the moderate (35%) yield observed in the oxidative cleavage of 2,3-dimethylindole. Because the dimer **4** is a requisite byproduct of

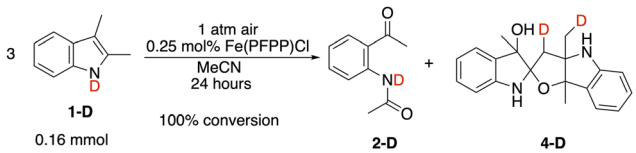

Scheme 5 The oxidation of *N*-D-2,3-DMI (**1D**) with air catalysed by Fe^{III}(PFPP)Cl in acetonitrile leads to the formation of **2-D** and dimer **4-D**.

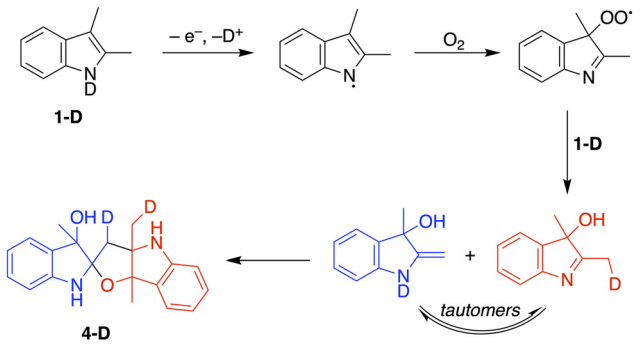

Scheme 6 Proposed mechanism for the formation of deuterated dimer (**4-D**) from a PCET oxidation of **1-D** based on literature reports for formation of **4**.[27–30] See ESI† for a more detailed mechanism.

the balanced reaction, the formation of this species accounts for two equivalents of every indole substrate added to the reaction. Therefore, the theoretical yield of **2** is actually only 33% of the original indole. Taking this theoretical maximum into account, the isolated yield of **2** (30%, see ESI†) is in fact a 91% yield.

By exploiting our understanding of the catalytic mechanism, we imagined being able to "turn on" reactivity for substrates that do not intrinsically undergo this reaction with ferric porphyrin. As an example, 3-methylindole does not exhibit reactivity under the same reaction conditions as 2,3-DMI (Scheme 7, top). This can possibly be explained by the slightly higher bond dissociation free energy (BDFE) of the N–H in 3-methylindole *versus* 2,3-DMI.[31] Because 3-methylindole is unable to reduce the iron porphyrin, it is unable to generate the iron superoxo intermediate necessary to enable oxidative cleavage. However, if we include an exogenous chemical reductant that can reduce the metal from iron(III) to iron(II), we should be able to enable reactivity with this substrate. Experimentally, in the presence of decamethylferrocene (Fc*) as the reductant, we observe partial conversion of 3-methylindole to the oxidative cleavage product (*N*-(2-acetylphenyl)formamide) in 49% NMR yield (Scheme 7, bottom). This finding highlights that we can enable reactivity of the ferric porphyrin by adding a reductant, allowing us to perform the oxidative cleavage of indoles that would otherwise be unreactive with the ferric porphyrin.

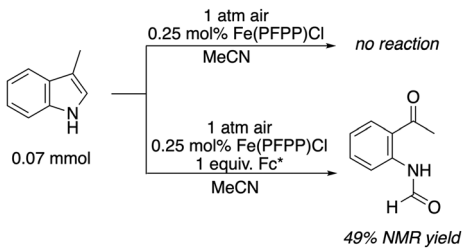

Scheme 7 Top: The oxidation of 3-methylindole does not occur with Fe^{III}(PFPP)Cl and air in acetonitrile. Bottom: The oxidation of 3-methylindole with air and decamethylferrocene (Fc*) catalysed by Fe^{III}(PFPP)Cl in acetonitrile leads to the formation of *N*-(2-acetylphenyl)formamide in 49% NMR yield.

Conclusions

This work demonstrates that with Fe(PFPP)Cl and Fe(TPP)Cl, the oxidative cleavage of 2,3-DMI occurs in the presence of only the ferric porphyrin and O_2. The data herein suggest 2,3-DMI reduces the Fe^{III}(porphyin) to Fe^{II}(porphyrin) through a PCET mechanism. This hypothesis is supported by UV-Vis spectra of the ferric porphyrin after reaction with both 2,3-DMI and the protected *N*-methyl-2,3-DMI as well as deuterium-labelling experiments. Subsequently, the Fe^{II}(porphyrin) is able to bind O_2 and generate the critical superoxo intermediate, which is observed as the catalyst resting state. The $Fe^{III}(O_2^{\bullet-})$(porphyrin) complex is then able to perform the oxidative cleavage reaction, as has been previously demonstrated stoichiometrically.[15,16]

The exploration of this mechanism allowed us to enable catalytic reactivity of 3-methylindole, a substrate that does not react with the iron(III) porphyrin. This mechanistic insight also highlights the importance of careful substrate selection in biomimetic systems. If this PCET reactivity is not accounted for, deleterious reactivity could occur and complicate the kinetics and conclusions of biomimetic studies.

Author contributions

ACB designed the project, oversaw all experiments, and aided in student data interpretation. JHL performed all experiments with the deuterated substrate. SEO performed experiments with 3-methylindole. ERS collected all UV-Vis spectra of 2,3-DMI with Fe(PFPP)Cl. OZ synthesized *N*-methyl-2,3-DMI, tested its reactivity, and measured UV-Vis spectra.

Conflicts of interest

There are no conflicts to declare.

Data availability

The data supporting this article have been included as part of the ESI.†

Acknowledgements

This work was supported by the donors of ACS Petroleum Research Fund under ACS-PRF Grant 65604-UNI1. We also thank both St Olaf College and Skidmore College for funding. We also thank Prof. James Mayer for use of his variable temperature UV-Vis spectrometer and glovebox.

References

1 A. A. Fatokun, N. H. Hunt and H. J. Ball, *Amino Acids*, 2013, **45**, 1319–1329.
2 M. Platten, W. Wick and B. J. Van Den Eynde, *Cancer Res.*, 2012, **72**, 5435–5440.
3 D. H. Munn, M. Zhou, J. T. Attwood, I. Bondarev, S. J. Conway, B. Marshall, C. Brown and A. L. Mellor, *Science*, 1998, **281**, 1191–1193.
4 T. L. Poulos, *Chem. Rev.*, 2014, **114**, 3919–3962.
5 M. L. Pegis, C. F. Wise, D. J. Martin and J. M. Mayer, *Chem. Rev.*, 2018, **118**, 2340–2391.
6 Y. H. Wang, P. E. Schneider, Z. K. Goldsmith, B. Mondal, S. Hammes-Schiffer and S. S. Stahl, *ACS Cent. Sci.*, 2019, **5**, 1024–1034.
7 T. Liu, H. Qin, Y. Xu, X. Peng, W. Zhang and R. Cao, *ACS Catal.*, 2024, **14**, 6644–6649.
8 T. Liu, J. Meng, H. Qin, M. Zhang, N. Sun, B. Mei, H. Li, X.-P. Zhang, J. Li and R. Cao, *J. Am. Chem. Soc.*, 2025, **147**, 22322–22328.
9 H. Qin, J. Kong, X. Peng, Z. Wang, X. Li, H. Lei, W. Zhang and R. Cao, *ChemSusChem*, 2025, **18**, e202401739.
10 Md. A. Hoque, J. B. Gerken and S. S. Stahl, *Science*, 2024, **383**, 173–178.
11 I. Efimov, J. Basran, S. J. Thackray, S. Handa, C. G. Mowat and E. L. Raven, *Biochemistry*, 2011, **50**, 2717–2724.
12 S. J. Thackray, I. Efimov, E. L. Raven and C. G. Mowat, in *Iron-Containing Enzymes: Versatile Catalysts of Hydroxylation Reactions in Nature*, ed. S. P. de Visser and D. Kumar, The Royal Society of Chemistry, 2011, ch. 12, pp. 400–426.
13 J. P. T. Zaragoza and D. P. Goldberg, in *Dioxygen-dependent Heme Enzymes*, ed. M. Ikeda-Saito and E. Raven, The Royal Society of Chemistry, 2018, pp. 1–36.
14 M. T. Nelp, V. Zheng, K. M. Davis, W. K. J. Stiefel and J. T. Groves, *J. Am. Chem. Soc.*, 2019, **141**, 15288–15300.
15 J. J. D. Sacramento and D. P. Goldberg, *Chem. Commun.*, 2020, **56**, 3089–3092.
16 P. Mondal and G. B. Wijeratne, *J. Am. Chem. Soc.*, 2020, **142**, 1846–1856.
17 M. Mukherjee and A. Dey, *Inorg. Chem.*, 2020, **59**, 7415–7425.
18 S. Samanta, S. Sengupta, S. Biswas, S. Ghosh, S. Barman and A. Dey, *J. Am. Chem. Soc.*, 2023, **145**, 26477–26486.
19 J. Rosenthal, B. J. Pistorio, L. L. Chng and D. G. Nocera, *J. Org. Chem.*, 2005, **70**, 1885–1888.
20 J. Rosenthal, T. D. Luckett, J. M. Hodgkiss and D. G. Nocera, *J. Am. Chem. Soc.*, 2006, **128**, 6546–6547.
21 E. Vanover, Y. Huang, L. Xu, M. Newcomb and R. Zhang, *Org. Lett.*, 2010, **12**, 2246–2249.
22 J. Jung, K. Ohkubo, K. A. Prokop-Prigge, H. M. Neu, D. P. Goldberg and S. Fukuzumi, *Inorg. Chem.*, 2013, **52**, 13594–13604.
23 J. Jung, K. Ohkubo, D. P. Goldberg and S. Fukuzumi, *J. Phys. Chem. A*, 2014, **118**, 6223–6229.
24 J. Jung, H. M. Neu, P. Leeladee, M. A. Siegler, K. Ohkubo, D. P. Goldberg and S. Fukuzumi, *Inorg. Chem.*, 2016, **55**, 3218–3228.
25 J. Pérez-Prieto, F. Boscá, R. E. Galian, A. Lahoz, L. R. Domingo and M. A. Miranda, *J. Org. Chem.*, 2003, **68**, 5104–5113.
26 M. L. Pegis, D. J. Martin, C. F. Wise, A. C. Brezny, S. I. Johnson, L. E. Johnson, N. Kumar, S. Raugei and J. M. Mayer, *J. Am. Chem. Soc.*, 2019, **141**, 8315–8326.
27 E. Leete, *J. Am. Chem. Soc.*, 1961, **83**, 3645–3647.
28 V. Dave and E. Warnhoff, *Can. J. Chem.*, 1971, **49**, 1911–1920.
29 S. McLean and G. I. Dmitrienko, *Can. J. Chem.*, 1971, **49**, 3642–3647.
30 X. Shen, J. Lind, T. E. Eriksen and G. Merényi, *J. Chem. Soc., Perkin Trans. 2*, 1990, 597–603.
31 R. G. Agarwal, S. C. Coste, B. D. Groff, A. M. Heuer, H. Noh, G. A. Parada, C. F. Wise, E. M. Nichols, J. J. Warren and J. M. Mayer, *Chem. Rev.*, 2022, **122**, 1–49.